Thin Solid Films, **518**, 537-540 (2009)

Improvement of stability for organic solar cells by using molybdenum trioxide buffer layer

Yoshihiro Kanai, Toshinori Matsushima, and Hideyuki Murata*

School of Materials Science, Japan Advanced Institute of Science and Technology,

1-1 Asahidai, Nomi, Ishikawa 923-1292, Japan

Abstract

We demonstrated that the stability of organic solar cells (OSCs) under light irradiation is markedly enhanced by inserting a molybdenum trioxide (MoO_3) buffer layer between an anode layer of indium tin oxide (ITO) and a *p*-type layer of 5,10,15,20-tetraphenylporphyrin (H_2TPP) or *N*,*N*'-di(1-naphthyl)-*N*,*N*'-diphenylbenzidine (α-NPD). The use of the MoO_3 layer also enhanced open-circuit voltages and power conversion efficiencies of the OSCs due to an increase in built-in potential. From results of stability test of hole-only α-NPD devices, we concluded that the OSC degradation occurs near the ITO/*p*-type layer interface and that the use of the MoO_3 layer can prevent the degradation at this interface.

Keywords: Organic solar cells, stability, degradation, molybdenum trioxide (MoO_3), interface of indium tin oxide (ITO) and α-NPD

* Corresponding author. Tel.: +81 761 51 1531; fax: +81 761 51 1149

E-mail address: murata-h@jaist.ac.jp (H. Murata)

1. Introduction

Organic solar cells (OSCs) are a promising candidate for generating renewable energy due to their potentials for use in mechanically flexible, light-weight, low-cost, and large-area applications. A very high power conversion efficiency (η_p) of ≈ 5 % was achieved in bulk heterojunction OSCs employing a polymer-fullerene (C_{60}) blend layer [1,2]. Recently, we have reported that use of a molybdenum trioxide (MoO_3) buffer layer with a high work function of -5.92 eV can improve open-circuit voltages (V_{oc}) from 0.57 V to 0.97 V, which in turn increases in η_p from 1.24% to 1.88% of an OSC using 5,10,15,20-tetraphenylporphyrin (H_2TPP) as a *p*-type layer and C_{60} as a *n*-type layer [3]. In addition to the improvement of the η_p, the enhancement of OSC stability is also required for the commercialization. Intensive research has been carried out to understand degradation mechanisms and improve the stability of polymer OSC [4]. On the other hand, the reports on the degradation mechanism of small molecular based OSCs are limited. For example, Norrman et. al. have reported that the oxygen/water degrade OSCs performances where diffusion process of oxygen/water into OSCs devices was investigated using time of flight-secondary ion mass spectrometry (TOF-SIMS) with isotopically labeled oxygen($^{18}O_2$) and water($H_2{}^{18}O$) [5].

One can notice that OSCs have many similarities with organic light-emitting diodes (OLEDs) in terms of the device structure. Thus, the knowledge of the degradation mechanism of OLEDs might be useful for understanding the degradation process of OSCs. Aziz et al. have reported that the degradation mechanisms for OLEDs and concluded that the one of major cause of degradation of OLEDs would be at the ITO and aluminum electrodes [6-8]. Recently, we have found that the stability of organic light-emitting diodes is markedly enhanced by inserting a MoO_3 hole-injection layer between the ITO and α-NPD [9].

In this work, we investigated how the use of a MoO_3 buffer layer between the ITO and the *p*-type layer affects the OSC stability. We found that the degradation of our OSCs mainly occurs near the ITO/*p*-type layer interface and that the use of the MoO_3 buffer layer can enhance the stability as well as the η_p.

2. Experimental

The OSC structures investigated in this study are shown in Figs. 1(a) and 1(b). The common OSC structure shown in Fig. 1(a) was composed of a glass substrate coated with a 150 nm anode layer of indium tin oxide (ITO) with a sheet resistance of 10 Ω/sq,

a 10 nm *p*-type layer, a 40 nm *n*-type C_{60} layer, a 10 nm exciton-blocking layer of 2,9-dimethyl-4,7-diphenyl-1,10-phenanthroline (BCP), and a 100 nm Ag cathode layer. Since V_{oc} is controlled by the difference in energy level between a highest occupied molecular orbital (HOMO) of a *p*-type layer and lowest unoccupied molecular orbital (LUMO) of a *n*-type layer [10], we used H_2TPP and *N*,*N*'-di(1-naphthyl)-*N*,*N*'-diphenylbenzidine (α-NPD) as a *p*-type layer due to their high HOMO energy levels (-5.5 eV for H_2TPP and -5.3 eV for α-NPD [11]). The OSCs were fabricated in the following ways: Glass substrates coated with an ITO layer were cleaned using ultrasonication in acetone, followed by ultrasonication in detergent, pure water, and isopropanol. The substrates were treated by UV ozone for 30 min and then annealed at 150˚C for 10 min in air. MoO_3 and organic layers were successively vacuum-deposited under a base pressure of 10^{-4} Pa on the cleaned ITO layer. To complete the OSC structures, an Ag layer was vacuum-deposited through a shadow mask to define the active area of the devices to be 4 mm^2. To investigate the degradation mechanisms of the OSCs, we also fabricated the hole-only devices with a glass substrate/ITO (150 nm)/MoO_3 (0 or 20 nm)/α-NPD (70 nm)/MoO_3 (10 nm)/Al (100 nm) structure. In the hole-only structures, we used a high-work-function MoO_3 layer (-5.7 eV [11]) at the α-NPD/Al interfaces to prevent injection of electrons from

the cathode. The deposition rates were 0.03 nm/s for MoO_3, H_2TPP, α-NPD, and C_{60}, 0.1 nm/s for BCP, and 0.3 nm/s for Ag and Al. Source materials of H_2TPP (Aldrich) and C_{60} (MTR, Ltd.) were purified twice using a temperature-gradient vacuum train sublimation technique before use. High-purity source materials of MoO_3 (6N grade, Mitsuwa Chemical), α-NPD (Nippon Steel Chemical), BCP (Nippon Steel Chemical), Ag (Nilaco), and Al (Nilaco) were used as received. The completed devices were transferred to a dry nitrogen-filled glove box (H_2O and O_2 concentrations less than 2 ppm) connected next to the vacuum evaporator and they were encapsulated with a glass cap and an ultraviolet curing epoxy resin. The changes of the current density-voltage (*J*-*V*) characteristics under dark and light irradiation conditions were measured at room temperature using a Keithley 2400 source measurement unit and an AM 1.5 Solar simulator (Eagle Engineering Corporation, Japan) at the light intensity of 100 mW/cm^2.

3. Results and discussion

Table I summarizes the initial device parameters of the short-circuit currents (J_{sc}), the V_{oc}, the fill factors (*FF*) and the η_p of the OSCs. The insertion of a MoO_3 layer between the ITO and the *p*-type layer led to an increase in V_{oc} from 0.80 V to 0.99 V for the H_2TPP and from 0.64 V to 0.87 V for the α-NPD. According to a

metal-insulator-metal model and a *p*-*n* junction model, the origin of V_{oc} is explained by two ways: (1) the difference in energy level between work functions of an anode and a cathode and (2) the difference in energy level between a HOMO of a *p*-type material and a LUMO of a *n*-type material [12-14]. Since depositing the MoO_3 on the ITO surface increases the work functions of the anodes [3], the increase in the V_{oc} is attributable to an increase in work function of the ITO/MoO_3 anodes. We also observed an increase in η_p by using the MoO_3 due to the increase in the V_{oc}.

Figure 2 shows the changes of the J_{sc}, the V_{oc}, the *FF*, and the η_p for the OSCs with the H_2TPP as a function of light irradiation time. While the OSCs with no buffer layer were drastically degraded with operational time, inserting the MoO_3 between the ITO and the H_2TPP suppressed the degradation. Although the η_p of the OSCs without the MoO_3 decreased to 37 % of its initial value after 60 min, the η_p of the OSC with the MoO_3 maintained 66 % of the initial value.

In addition to the H_2TPP OSCs, we investigated the stability of the α-NPD OSCs (Fig. 3). The η_p of the α-NPD OSC with the MoO_3 maintained 100 % of the initial value, while the α-NPD device without the MoO_3 decreased to 46 % of its initial

value. In this device, we observed a slight increase in J_{sc}, *FF*, and η_p of the OSCs with the MoO_3 after the light irradiation. The origin of the increase in these parameters is not clear. As described later, we observed the similar increase of the dark current density in the hole-only α-NPD devices after the light irradiation. One of the possible explanations of the increase in the J_{sc} might be caused by a heating effect due to the light irradiation [4]. These results clearly indicate that inserting the MoO_3 layer markedly improved the OSC stability and suggests that the degradation of the OSCs mainly occurs at the ITO/*p*-type layer interfaces (*Vide infra*).

To get insights at the anode/α-NPD interfacial degradation, we fabricated the hole-only α-NPD devices. This structure can reduce the number of unnecessary interface (see the structures shown in the insets of Figs. 4(a) and 4(b)). Figure 4 shows the changes of the *J*-*V* characteristics of the hole-only devices during the light irradiation. The α-NPD device without the MoO_3 layer was markedly degraded by the light irradiation. The current density at the forward bias, where ITO electrode was biased positively, significantly dropped to 0.7% of its initial value while the current density at the reverse bias became unchanged. On the other hand, we observed no degradation in the device with the MoO_3 layer in both forward and reverse bias

directions after the light irradiation. Again, we observed that the slight increase in current density by the light irradiation. These results suggest that the decrease in the current density in the forward bias region is not caused by an increase in resistance of the α-NPD bulk layer but is caused by an increase in hole injection barrier height between the ITO and the α-NPD after the light irradiation. In other words, the relative position of the HOMO level of the α-NPD to the Fermi level of the ITO might be shifted to the direction of increasing the hole injection barrier height after the light irradiation. We attribute the shift of the relative energy level position to a vacuum level shift caused by a chemical reaction between the ITO and the α-NPD [15,16]. Moreover, the difference in energy level between the Fermi levels of the ITO and the Ag would be reduced by the vacuum level shift. In this event, the built-in potential of the OSCs decreases, resulting in the reduction of the V_{oc}. The insertion of the MoO_3 would prevent this reaction and, therefore, enhance the device stability.

4. Summary

We have demonstrated that the stability of OSCs using H_2TPP and α-NPD as a *p*-type layer under light irradiation is enhanced by inserting a MoO_3 layer between ITO and the *p*-type layer. The insertion of the MoO_3 layer also enhanced V_{oc} and η_p of the

OSCs due to an increase in built-in potential. To clarify the mechanism of the enhanced stablity, we investigated the stability of hole-only α-NPD devices. While the hole-only device without the MoO_3 layer between ITO and the *p*-type layer exhibited a dramatic decrease in current density in a forward bias region, *J-V* characterisics of the hole-only device with the MoO_3 layer were not changed after light irradiation. From these results, we concluded that the OSC degradation occurs near the ITO/α-NPD interface by light irradiation and that the MoO_3 layer can prevent the degradation at this interface.

References

[1] W. Ma, C. Yang, X. Gong, K. Lee, A. J. Heeger, Adv. Funct. Mater. 11 (2005) 1617.

[2] G. Li, V. Shrotriya, J. Huang, Y. Yao, T. Moriarty, K. Emery, Y. Yan, Nat. Mater. 4 (2005) 864.

[3] Y. Kinoshita, R. Takenaka, H. Murata, Appl. Phys. Lett. 92 (2008) 243309.

[4] M. Jørgensen, K. Norrman, F. C. Krebs, Sol. Energy Mater. Sol. Cells 92 (2008) 686.

[5] K. Norrman, F. C. Krebs, Surf. Interface Anel. 36 (2004) 1542.

[6] H. Aziz, G. Xu, Synth. Mat. 80 (1996) 7.

[7] H. Aziz, Z. D. Popovic, N. –X. Hu, A. Hor, G. Xu, Science 283 (1999) 1900.

[8] H. Aziz, Z. D. Popovic, Chem. Mater. 16 (2004) 4522

[9] T. Matsusihima, H. Murata, J. Appl. Phys. 104 (2008) 034507.

[10]C.-W. Chu, Y. Shao, V. Shrotriya, Y. Yang, Appl. Phys. Lett. 86 (2005) 243506.

[11] We measured work functions and ionization potential energies of vacuum-deposited layers of H_2TPP (50 nm), α-NPD (50 nm), and MoO_3 (10, 20, and 50 nm) on ITO using ultraviolet photoelectron spectroscope (AC-2, Riken Keiki Co.). The measured values were -5.0 eV for ITO, -5.3 eV for α-NPD, -5.5

eV for H_2TPP, -5.7 eV for 10 nm MoO_3, -5.8 eV for 20 nm MoO_3, and -5.9 eV for 50 nm MoO_3.

[12] V. D. Mihailetchi, P. W. M. Blom, J. C. Hummelen, M. T. Rispens, J. Appl. Phys. 94 (2003) 6849.

[13] C. J. Brabec, A. Cravino, D. Meissner, N.S. Sariciftci, T. Fromherz, M. T. Rispens, L. Sanchez, J. C. Hummelen, Adv. Funct. Mater. 11 (2001) 374.

[14] C. J. Brabec, Sol. Energy Mater. Sol. Cells 83(2004) 273.

[15] K. Akedo, A. Miura, K. Noda, H. Fujikawa, Proceedings of the 13th International Display Workshops (2006) 465.

[16] H. Ishii, K. Sugiyama, E. Ito, K. Seki, Adv. Mater. 11 (1999) 605.

Table I. Summary of J_{sc}, V_{oc}, *FF*, and η_p of our OSCs.

OSC structure	J_{sc} (mA/cm^2)	V_{oc} (V)	*FF*	η_p (%)
ITO/H_2TPP	-3.09	0.80	0.58	1.44
ITO/MoO_3/H_2TPP	-2.98	0.99	0.58	1.70
ITO/α-NPD	-2.61	0.64	0.56	0.93
ITO/MoO_3/α-NPD	-2.46	0.87	0.46	1.00

Figure captions

Fig. 1. Schematics of OSC structures (a) without MoO_3 and (b) with MoO_3. As *p*-type layer, we used H_2TPP and α-NPD.

Fig. 2. Changes of (a) V_{oc}, (b) J_{sc}, (c) *FF*, and (d) η_p for H_2TPP OSCs with and without MoO_3 buffer layer under light irradiation.

Fig. 3. Changes of (a) V_{oc}, (b) J_{sc}, (c) *FF*, and (d) η_p for α-NPD OSCs with and without MoO_3 buffer layer under light irradiation.

Fig.4. Change of *J*-*V* characteristics of α-NPD hole-only devices (a) without MoO_3 and (b) with MoO_3 under light irradiation. Insets show structures of hole-only devices.

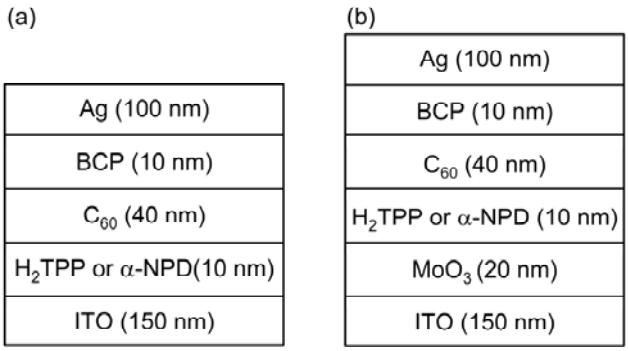

Figure 1

Kanai *et al.*

Thin Solid Films

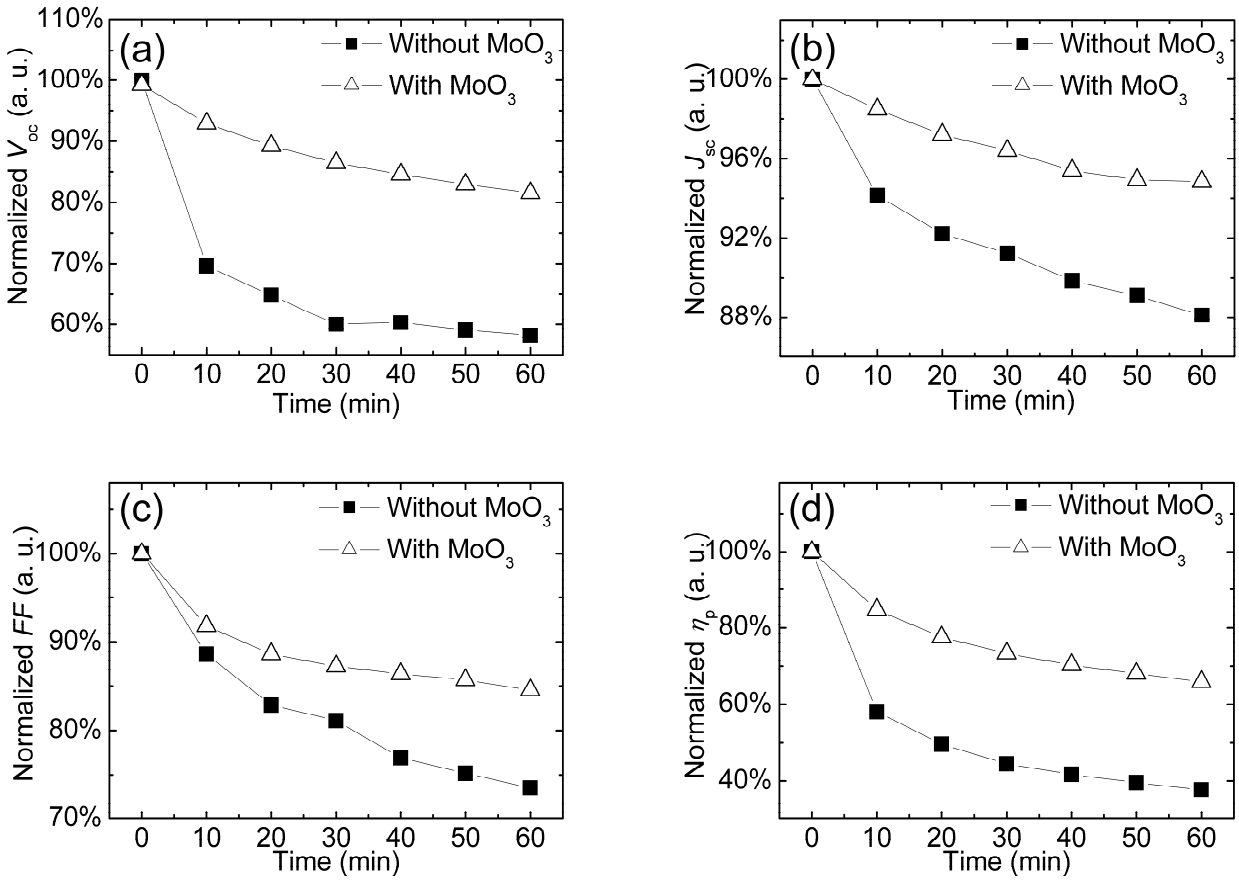

Figure 2

Kanai *et al.*

Thin Solid Films

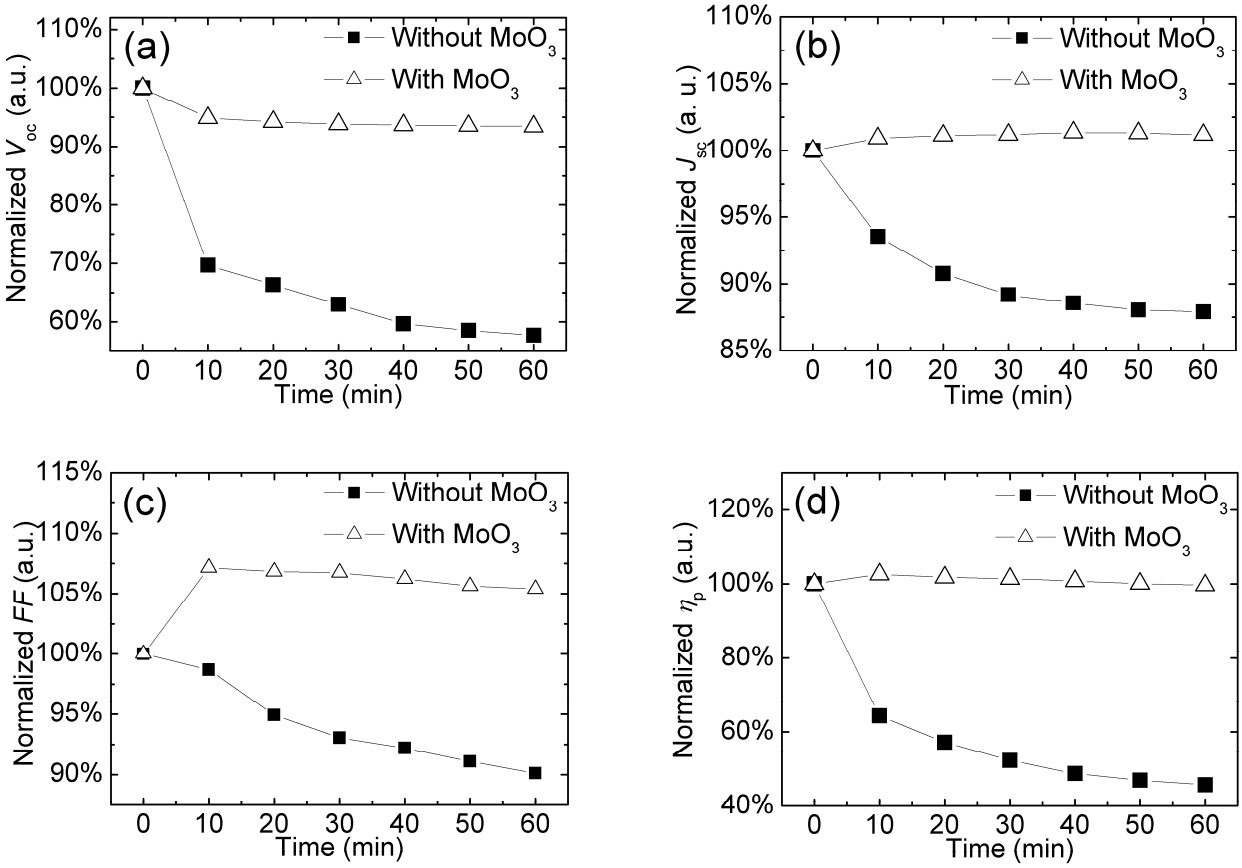

Figure 3

Kanai *et al.*

Thin Solid Films

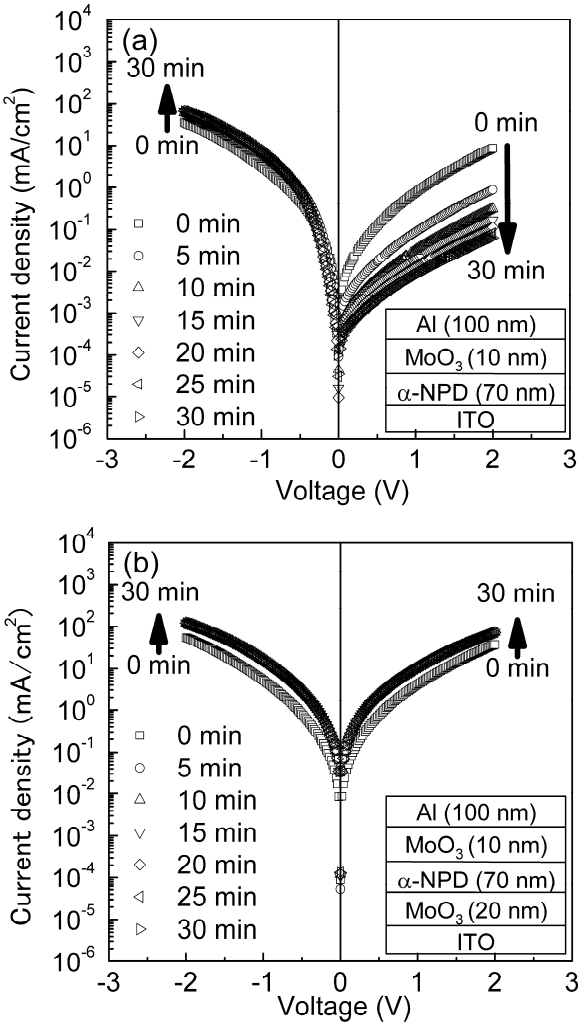

Figure 4

Kanai *et al.*

Thin Solid Films